SCIENTIFIC AND RESOURCE CHARACTERIZATION OF LUNAR REGOLITH USING DIELECTRIC SPECTROSCOPY. D. E. Stillman and R. E. Grimm, Department of Space Studies, Southwest Research Institute, 1050 Walnut Street, Suite 300, Boulder, CO 80302, dstillman@boulder.swri.edu, grimm@boulder.swri.edu.

Introduction: Water ice and ilmenite both have unique dielectric responses that can be used to detect their concentration as a function of depth, noninvasively from the lunar surface. Electrical measurements at the surface can also be used to determine the density of the lunar regolith. Subsurface water ice may exist in permanently shadowed regions near the poles of the Moon [1-6]. The presence of water in these permanently shadowed areas is not only important for in-situ resource utilization (ISRU), but it also records the flux of volatiles into the inner solar system over the last billion years. Ilmenite in the lunar regolith is an important part of ISRU for oxygen production. The vertical density profile determines the thickness of the lunar regolith.

Lunar Regolith: Previous measurements of lunar regolith showed that the high frequency part of the real part of the dielectric constant was directly related to the density via 1.9 where equals bulk density [7]. The lunar regolith was shown to contain a large dielectric relaxation at low frequencies that was proportional to its [TiO2%+FeO%] or ilmenite concentration [7]. This relaxation was found to relax over a broad frequency range (broad distribution of time constants) and to be temperature dependent with an activation energy of 2.5 eV [7]. At cold temperatures in the permanently shadowed regions of the Moon, this relaxation will shift out of the measurable frequency range. However, it can be measured at typical lunar temperatures.

Formation of Water Ice: It is believed that water ice and possibly CO_2 ice are transported to the Moon via comets and/or planetary outgassing. Water ice could also have formed from the regolith via impact vaporization, photon stimulated desorption, and ion sputtering. Once water condenses on the surface, it will stay there until it sublimates away. The sublimation rate is extremely temperature dependent varying exponentially with increasing temperature. For example, water ice will sublimate away at a rate of 1 m per a billion years at a temperature of 110 K [8]. Stable water ice deposits are typically modeled with temperatures below 110 K and only occur in the permanently shadow regions [8]. When deposited, the water ice is in the form of amorphous ice. Even at these cold temperatures amorphous ice will convert to cubic ice over millions of years [9].

Two groups have measured the electrical properties of cubic ice. Unfortunately, their conclusions varied. Gough and Davidson [10] found that the relaxation frequency of cubic ice and hexagonal ice were the same, while Johari [11] found that cubic ice had an order of magnitude higher relaxation frequency than hexagonal ice. We plan to measure cubic ice in the future, but are currently concentrating on measuring hexagonal ice.

Dielectric Relaxation of Hexagonal Ice: Dispersion in the dielectric constant arises from frequency dependence in polarizability and is often manifested as a distinct band of maximum change, a dielectric relaxation (Fig. 1). Bjerrum defects in water ice are strongly polarized at low frequencies to create a real part of the relative dielectric permittivity at low frequency ($'_{DC}$) >90. At high frequency, these defects cannot move fast enough to polarize fully, limiting the real part of the dielectric constant to ~3. The Debye relaxation frequency occurs at the frequency where these defects are in constant motion.

The relaxation frequency and $'_{DC}$ are dependent on temperature, the amount of excess H^+ and OH^-, and the amount of Cl^- and F^- impurities that have replaced O^{2-} in the lattice structure of ice [12]. Due to the lack of Cl^- and F^- on the Moon, we believe the ice will be relatively pure. The temperature dependence of the relaxation frequency follows an Arrehenius relationship with an activation energy of 0.56 eV. Impurities cause the activation energy to reduce to 0.23 eV at low temperatures. Even double and triple deionized water ice has been shown to shift to this lower activation energy at around 233 K [14,15]. The value of activation energy describes how quickly relaxation frequency changes with temperature.

Laboratory Measurement: The dielectric relaxation of pure and doped ice has been measured previously; however much uncertainty remains in these measurements at temperatures below 213 K [13-15]. Minimal research has been conducted on the effects of ice in soil [16,17]. Extrapolations from existing data show that the ice relaxation at the temperature of the permanently shadowed lunar craters (100 K) is most likely greater than 10^{-5} Hz (Fig 2). To reduce this uncertainty, we have been making temperature and frequency dependent electrical property measurements of soil/ice mixtures as well as pure and doped ice samples over a temperature range from 90 – 273 K and frequency range from 1 mHz – 1 MHz. Electrical properties measurements are being made with a 1260 Solartron Impedance Analyzer connected to a 1296 Dielectric Interface or a 1294 Impedance Interface. Measurements are made in a three-electrode geometry [e.g., 18]. Electrical properties can be expressed as complex dielectric constant, complex conductivity, or complex resistivity.

Application: Narrowband measurement of the resistive-capacitive properties of the earth ("induced polarization") has been used for nearly a century to explore for minerals and groundwater and to characterize subsurface geology. Broadband systems are now seeing wide application, including environmental studies [e.g., 19]. The Huygens, the Rosetta lander, and Phoenix spacecraft all include electrical-properties sensors. However, characterization of the full bandwidth of possible water-ice responses and soundings to depths of meters or more requires high-impedance (~10 T), low-capacitance (~1 pF) coupling, mitigation of coherent noise such as leakage and eddy currents using buffering shielding, guarding of electrodes, and larger electrode arrays. The electrodes (sensors) can be accommodated in lander legs, rover wheels, a robotic arm, or in a ballistically deployed string (Fig 1). Our present efforts are aimed toward a design of a transmitter and receiver requiring a few kilograms and a few watts, plus sensors.

A forward calculation using present estimates of the intrinsic properties of ice and its moderation due to regolith mixing (Fig. 2) illustrates that an ice-detection limit of ~1% or better is possible.

References: [1] Nozette, S. et al. (1996) *Science, 274*, 1495-1498. [2] Vasavada, A.R. et al. (1999) *Icarus, 141*, 179-193. [3] Feldman, W.C. et al. (2001) *JGR, 106*, 23231-23252. [4] Nozette S. et al. (2001) *JGR, 106*, 23253-23266. [5] Feldman, W.C. (2002) *Science, 197*, 75-78 [6] Campbell, D.B. et al. (2006) *Nature, 443*, 835-837. [7] Carrier, W.D. et al. (1991) in *Lunar Sourcebook (eds. Heiken et al.)*, 475-594. [8] Vasavada, A.R. et al. (1999) *Icarus, 141*, 179-193. [9] Kouchi, A. et al., (1994) *Astron. Astrophys., 290*, 1009-1018. [10] Gough and Davidson (1970) *Journ. Chem. Phys., 52*, 5442-5449. [11] Johari, G.P. et al. (1991) *Journ. Chem. Phys., 52*, 2955-2964. [12] Petrenko V.F. and Whitworth R.W. (1999) *Physics of Ice*, 373 pp. [13] Auty, R.P. and Cole R.J. (1952) *J. Chem. Phys., 20*, 1309. [14] Kawada, S. (1978) *J. Phys. Soc. Jpn.*, 44, 1881-1886. [15] Johari G.P. and Whalley E. (1981) *J. Chem. Phys., 75*, 1333-1340. [16] Alvarez R. (1973) *Earth & Planet. Sci. Let., 20*, 409-414. [17] Alvarez R. (1973) *Science, 179*, 1122-1123. [18] Olhoeft, G.R. (1985), *Geophys*., 50, 2492-2503. [19] Grimm R.E. (2005) *J. Environ. Eng. Geophys., 10*, 351-364. [20] Telford W.M. et al. (1990) *Applied Geophysics*, 770 pp.

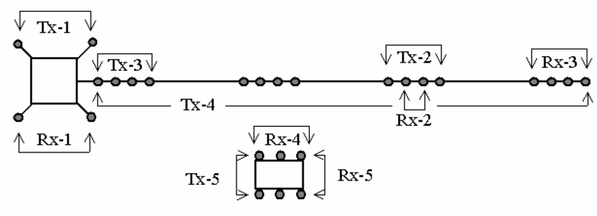

Figure 1. Alternative schematic layouts for IP electrodes. Tx = transmitter, Rx = receiver. (1) Electrodes on static lander footpads. (2) Closely spaced electrodes on ballistically deployed string for shallow subsurface investigation. (3) Widely spaced electrodes for deeper investigation. (4) Large transmitter dipole on lander and short dipole on rover (wheel base) for deep investigation. (5) Rover-only short dipoles for mobile, shallow investigation.

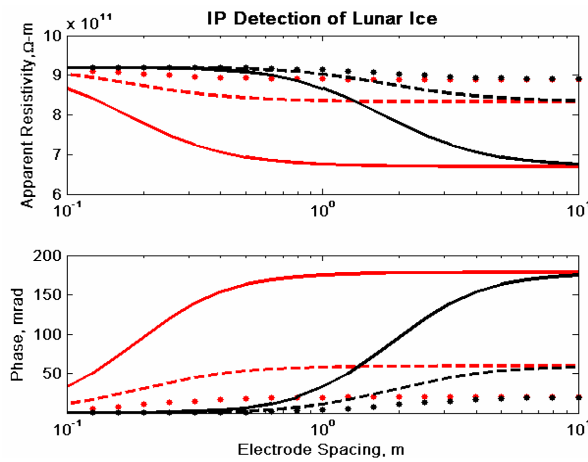

Fig. 2. Forward models for the geoelectrical signature of lunar ice from surface electrode arrays. Model invokes a two-layered structure [20], uses the complex refractive index model (CRIM) to calculate electrical properties of mixtures of soil and the target substance, and assumes that multiple electrodes are distributed along a linear antenna such that four-electrode combinations can be used at a variety of spatial scales. Ice depths of 0.1 m (red) and 1 m (black) and ice fractions 10% (solid), 3% (dash), and 1% (dot) indicate that ice can be resolved at percent abundance or better (relaxation time constant of ice after Kawada [14]; dry regolith resistivity 10^{12} -m after Carrier et al. [7]; test frequency 1 mHz).